Topology in the space-time scaling limit of quantum dynamics

Letter

Topology in the space-time scaling limit of quantum dynamics

Lorenzo Rossi [1,*] Jan Carl Budich,[2] and Fabrizio Dolcini [1]

[1]*Dipartimento di Scienza Applicata e Tecnologia, Politecnico di Torino, 10129 Turin, Italy*

[2]*Institute of Theoretical Physics, Technische Universität Dresden and Würzburg-Dresden Cluster of Excellence ct.qmat, 01062 Dresden, Germany*

(Received 19 January 2023; revised 26 May 2023; accepted 30 May 2023; published 7 June 2023)

We investigate the role of topology in the space-time scaling limit of quantum quench dynamics, where both time and system size tend to infinity at a constant ratio. There, while the standard topological characterization relying on local unitary transformations becomes ill defined, we show how a different dynamical notion of topology naturally arises through a dynamical winding number encoding the linear response of the Berry phase to a magnetic flux. Specifically, we find that the presence of a locally invisible constant magnetic flux is revealed by a dynamical staircase behavior of the Berry phase, whose topologically quantized plateaus characterize the space-time scaling limit of a quenched Rice-Mele model. These jumps in the Berry phase are also shown to be related to the interband elements of the DC current operator. We outline possible experimental platforms for observing the predicted phenomena in finite systems.

DOI: 10.1103/PhysRevB.107.L241402

Topology has become a cornerstone for understanding and distinguishing phases of matter [1–3]. While, initially, this approach was mostly used to unravel the topological properties of low-temperature systems [4–9], recent advances in experimentally controlling the quantum dynamics of atomic many-particle states [10,11] have triggered the study of topological features far from equilibrium. In particular, within the paradigmatic quantum quench protocol [12], new dynamical topological invariants, which are predicted to characterize the change in topology of the quenched Hamiltonian [13–18], have been observed [19,20], and the dynamical robustness of topological features has been addressed, both theoretically [21–29] and experimentally [30]. Since topological phases may be defined as equivalence classes under local unitary transformations [31], bulk topological properties of a quantum state cannot dynamically change during coherent time evolution generated by a local Hamiltonian [11,17,21,22,25,31]. Notwithstanding these fundamental constraints, symmetry-protected topological invariants can be fragile if the underlying symmetries are dynamically broken [28–30]. In addition, topological invariants are typically defined in the thermodynamic limit (TL), while all experiments deal with finite systems. Hence, the conventional topological characterization is meaningful only for timescales such that $t \ll L/v^f$, where L measures the system size and v^f is a characteristic band velocity of the postquench Hamiltonian [11]. At later times, since an extensively long unitary time evolution is no longer a local transformation, standard topological properties are expected to become ill defined [11], and previous works on quantum quenches have thus mostly focused on the $t \ll L/v^f$ regime. Alternatively, the opposite regime $t \gg L/v^f$ has been addressed in the context of adiabatic state preparation, where the finite size is harnessed to adiabatically connect different equilibrium topological phases [32–36].

In the present work we propose to investigate a different out-of-equilibrium regime, namely, the quench dynamics in the space-time scaling limit (STSL), where *both* time and system size tend to infinity while their ratio $\eta = 2\pi t/L$ is kept constant, and we show how a different dynamical topological invariant $\nu(\eta)$ naturally arises (see Fig. 1 for an illustration with a quenched Rice-Mele model [37,38]). To understand its physical implications, we analyze the effect of a constant magnetic flux Φ threading a one-dimensional (1D) system with periodic boundary conditions (PBCs). Remarkably, while Φ, as a global property, remains invisible in the quench dynamics for subextensive times, in the STSL the Berry phase [38–40] is found to dynamically acquire a staircase behavior (see Fig. 2), whose plateau values are topologically quantized as $2\pi\nu\Phi/\Phi_0$, where $\Phi_0 = h/e$ is the flux quantum. Since the limits $t \to +\infty$ and $L \to +\infty$ do not commute, these properties are unique to the STSL regime and cannot be obtained by applying the long time limit to formulas derived in the standard TL. However, we demonstrate that clear signatures of our predictions can be observed in finite systems of moderate size that are within reach of present-day quantum simulators.

For definiteness, we consider a sudden quench in a system of noninteracting spinless fermions hopping in a 1D bipartite lattice with PBCs, and we assume the Hamiltonian is traceless. We measure lengths in units of the lattice spacing a, so that the length L of the system coincides with the number of cells. Thanks to translation invariance we can write the initial and final realizations in reciprocal space as $H^{i/f} = \sum_k c^\dagger(k)[\mathbf{d}^{i/f}(k)\cdot\boldsymbol{\sigma}]c(k)$. Here $k \in 2\pi n/L$ is a dimensionless quasimomentum, where $n \in \{-\lfloor L/2\rfloor, \ldots, \lfloor (L-1)/2\rfloor\}$,

*lorenzo.rossi@polito.it

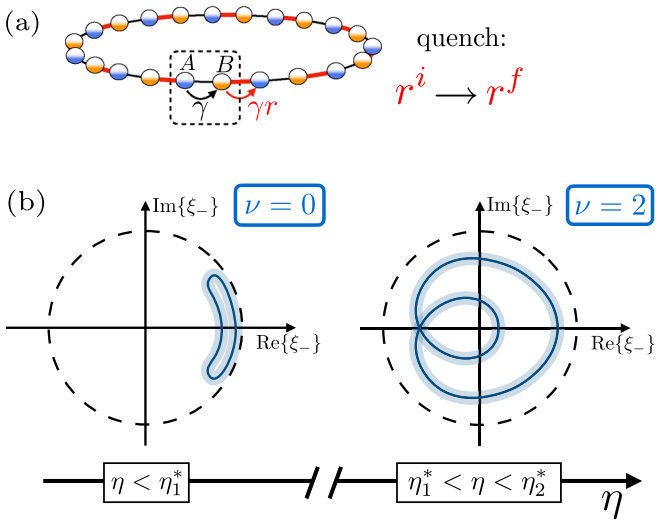

FIG. 1. (a) Illustration of a Rice-Mele lattice model on a ring [see Eq. (6)], subject to a quench by a sudden variation of the intercell hopping amplitude $\gamma r^i \to \gamma r^f$. (b) Schematic representation of the closed loops formed in the complex plane by the Bloch state overlap ξ_- [see Eq. (1)] as a function of quasimomentum k. Nontrivial loops (right panel) may form in the STSL regime at critical values η_m^* [see Eq. (3)] of the ratio $\eta = 2\pi t/L$. Solid lines represent the zeroth-order contribution $\xi_-^{(0)}(k,\eta)$ [see Eq. (2)]; shaded areas visualize the subleading contribution $2\pi\xi_-^{(1)}(k,\eta)/L$. When $\eta < \eta_1^*$ (left panel), the winding number ν vanishes, while for $\eta_1^* < \eta < \eta_2^*$ (right panel) $\nu = 2$. The dashed line depicts the unit circle as a guide to the eye.

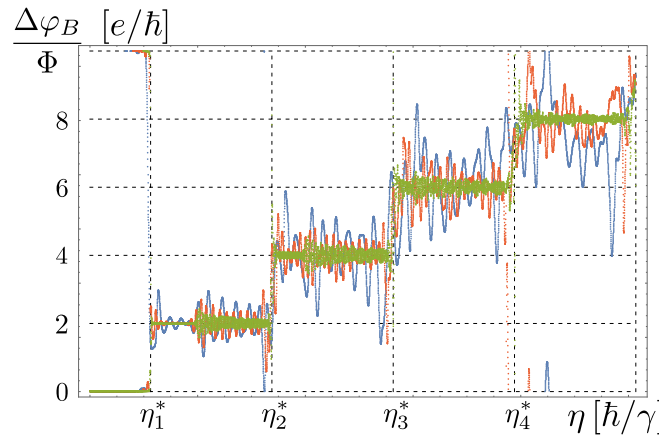

FIG. 2. The linear response $\Delta\varphi_B/\Phi$ of the Berry phase to an applied magnetic flux is plotted, in units of $e/\hbar = 2\pi/\Phi_0$, as a function of $\eta = 2\pi t/L$ in the STSL regime after quantum quenches in finite Rice-Mele lattices with PBCs [see Eq. (6)]. In all quenches, the energy scale γ is fixed to a constant value throughout the entire protocol, together with the ratio of the staggered potential $u = 0.1$. The ratio r of the staggered hopping amplitudes is instead quenched from $r^i = 0.5$ to $r^f = 2$, while the magnetic flux, when present, is constant and equal to $\Phi/\Phi_0 = 1/10$. System sizes are $L = 40$ (blue), $L = 80$ (red), and $L = 400$ (green). The plateaus at $\nu = 2, 4, 6$, and 8 are clearly visible already for $L = 40$; they do not depend on system size and abruptly change at critical ratios η_m^*. The fluctuations are, instead, system size dependent and are suppressed with increasing L.

while $\boldsymbol{\sigma}$ is the three-dimensional vector of Pauli matrices and $c^\dagger(k) = (c_A^\dagger(k), c_B^\dagger(k))$ is a spinor of fermionic operators, which create spinless fermions with quasimomentum k in sublattice A or B. All the information about the specific Hamiltonian realizations is thus encoded in the k-dependent three-dimensional vectors $\mathbf{d}^{i/f}(k)$. In particular, the initial and final spectra are given by $\epsilon_\pm^{i/f}(k) = \pm|\mathbf{d}^{i/f}(k)|$. Moreover, the time-evolved many-particle state can be easily reconstructed out of the single-particle time-dependent Bloch spinors $|u_\pm(k,t)\rangle = e^{-i[\mathbf{d}^f(k)\cdot\boldsymbol{\sigma}]t/\hbar}|u_\pm^i(k)\rangle$, where $|u_\pm^i(k)\rangle$ are the Bloch single-particle eigenstates of H^i.

We assume H^i has a finite band gap, initialize the system in its half-filled insulating ground state, and follow the time evolution of the Berry phase in its discretized formulation, appropriate for finite system sizes $\varphi_B(t,L) = \sum_k \arg\xi_-(k,t,L)$ [41], where

$$\xi_-(k,t,L) = \langle u_-(k+\delta k,t)|u_-(k,t)\rangle \tag{1}$$

and $\delta k = 2\pi/L$. As in the standard continuous formulation, the discrete Berry phase is gauge invariant under $|u_-(k,t)\rangle \to |u_-^\lambda(k,t)\rangle = e^{i\lambda(k)}|u_-(k,t)\rangle$ and takes quantized values, equal to either 0 or π, when charge conjugation symmetry is present [2,38,42]. Moreover, in the usual TL, i.e., $L \to +\infty$ while $t \in \mathbb{R}$, it is straightforward to realize that $\xi_-(k,t,L) = 1 + iA_B(k,t)\delta k + O(L^{-2})$, where $A_B(k,t) = \langle u_-(k,t)|i\partial_k|u_-(k,t)\rangle$ is the time-dependent Berry connection, and the standard result $\varphi_B(t) = \int_{-\pi}^{\pi} dk\, A_B(k,t)$ is recovered [38].

However, in the STSL, when $t, L \to +\infty$ with fixed $\eta = \delta k\, t = 2\pi t/L \in \mathbb{R}$, the function $\xi_-(k,t,L)$ may develop a nontrivial dependence on k and η already to zeroth order in the $1/L$ expansion. Indeed, one can write $\xi_-(k,t,L) = \xi_-^{(0)}(k,\eta) + \xi_-^{(1)}(k,\eta,t)\delta k + O(L^{-2})$, where [42]

$$\xi_-^{(0)}(k,\eta) = \cos[v^f(k)\eta] - i\,\mathcal{C}(k)\sin[v^f(k)\eta]. \tag{2}$$

Here $\mathcal{C}(k) = \hat{\mathbf{d}}^i(k)\cdot\hat{\mathbf{d}}^f(k)$ is the cosine of the k-dependent angle between the initial and final unit vectors, while $v^f(k) = \partial_k\epsilon_+^f(k)/\hbar$ is the postquench band velocity. Then it is straightforward to derive $|\xi_-^{(0)}(k,\eta)| = \sqrt{1 - \{\mathcal{S}(k)\sin[v^f(k)\eta]\}^2}$, where $\mathcal{S}^2(k) = 1 - \mathcal{C}^2(k)$, and we notice that, if $\mathcal{C}(k) = 0$ is satisfied by some k^*, Eq. (2) vanishes at equally spaced critical ratios

$$\eta_m^* = \left(\frac{\pi}{2} + (m-1)\pi\right)\frac{1}{v^f(k^*)}, \quad m \in \mathbf{N}_+. \tag{3}$$

Some comments are in order. In the limit $\eta \to 0$ one has $\xi_-^{(0)}(k,\eta) \to 1 + O(L^{-1})$, and the standard TL result is recovered. Moreover, at finite η, Eq. (2) is reminiscent of the k-dependent contribution to the Loschmidt amplitude, appearing in the context of dynamical quantum phase transitions (DQPTs) [13,14,43]. Similarly, the condition $\mathcal{C}(k^*) = 0$ leading to a vanishing $\xi_-^{(0)}$ in Eq. (2) is formally equivalent to the requirement for observing DQPTs [13]. However, we emphasize that, while the k-dependent contribution to the Loschmidt amplitude stems from the overlap between the initial and time-evolved Bloch spinors at the same k, the quantity studied here, Eq. (1), is the overlap between Bloch spinors that are *both* time evolved and that are computed at *different*

quasimomenta, namely, k and $k+\delta k$. It is precisely such a tiny deviation that yields Eq. (2) at $t \sim L/v^f$. Thus, while DQPTs occur at *finite* times in a TL system, Eq. (2) vanishes at *extensive* critical times $t_m^* = \eta_m^* L/2\pi$, with η_m^* given by Eq. (3).

We now start to investigate the topological features unique to the STSL regime, i.e., where η takes finite values even for arbitrarily large systems. Far away from its critical values, by treating η as a parameter, we can define $\alpha^{(0)}(k;\eta) = \arg \xi_-^{(0)}(k,\eta)$. The function $k \mapsto \alpha^{(0)}(k;\eta)$ from a circle to a circle naturally leads to the definition of a dynamical winding number $\nu(\eta) \in \mathbb{Z}$ through $\alpha^{(0)}(k;\eta) = \tilde{\alpha}^{(0)}(k;\eta) + k\,\nu(\eta)$, where $\tilde{\alpha}^{(0)}(k;\eta)$ is an $\mathbb{R}$-valued smooth periodic function. Remarkably, by contrast to the conventional equilibrium framework [2], this dynamical winding number does not require any symmetry to be properly defined. We can then write the Berry phase in the STSL regime as $\varphi_B(\eta) = \varphi_B^{(0)}(\eta) + \varphi_B^{(1)}(\eta)$, where

$$\varphi_B^{(0)}(\eta) = \frac{L}{2\pi}\int_{-\pi}^{\pi} dk\,[\tilde{\alpha}^{(0)}(k;\eta) + k\,\nu(\eta)], \tag{4}$$

while $\varphi_B^{(1)}(\eta)$ is analogous to the usual integral of the Berry connection [42]. Thus, let us focus on the consequences of the contribution stemming from a nontrivial $\xi_-^{(0)}$. *A priori*, $\varphi_B^{(0)}(\eta)$ is of order L, and given that the Berry phase is defined mod 2π, the zeroth order would produce a Berry phase that wildly fluctuates with time. Nonetheless, if $\mathbf{d}^i(k)$ and $\mathbf{d}^f(k)$ have the same parity under $k \leftrightarrow -k$, then $\alpha^{(0)}(k;\eta)$ becomes an odd function of k, and the integral in Eq. (4) vanishes identically. This condition physically corresponds to a quench that does not generate any stationary current [44]. However, if we now assume that a finite and constant magnetic flux Φ is present throughout the entire quench dynamics, the quasimomenta get shifted according to $k \to k+\phi$, where $\phi = \frac{2\pi}{L}\frac{\Phi}{\Phi_0}$. This shift does not affect the integral of the odd periodic part $\tilde{\alpha}^{(0)}(k;\eta)$, which remains vanishing. However, although ϕ is infinitesimal for large L, the shift yields a finite contribution proportional to $\nu(\eta)$, thanks to the factor L in Eq. (4). We thus end up with

$$\varphi_B^{(0)}(\eta;\Phi) = 2\pi\,\nu(\eta)\Phi/\Phi_0 + O(L^{-1}). \tag{5}$$

We can therefore conclude that, in the STSL, the Berry phase develops a nontrivial zeroth-order contribution which induces a quantized response to an applied magnetic flux and the quantization is encoded in the dynamical topological invariant $\nu(\eta)$. In this respect, ν plays a role analogous to the Chern number in the integer quantum Hall effect [4,5]: while the latter uniquely defines the linear Hall response to an applied electric field, the former encodes the linear response of the Berry phase to an applied magnetic flux. However, while the various plateaus in the Hall conductance identify different equilibrium topological phases as a function of the chemical potential, the winding number $\nu(\eta)$ topologically characterizes an out-of-equilibrium state and is thus a function of time. Note that, since $\nu(\eta)$ can change only at the critical ratios η_m^* in Eq. (3), the topological invariant is stable for *extensive* time windows $\Delta t = L/2v^f(k^*)$. This means that the system undergoes a new kind of dynamical topological phase transition, where a well-defined topological invariant suddenly changes at the extensive critical times t_m^*. Moreover, since the quantized response does not depend on system size, it is remarkable to note that even a fraction of the elementary flux quantum may yield a detectable signature in the coherent dynamics of a macroscopic quantum system.

After the above general derivations, we now choose a specific setup to illustrate our results. We consider a sudden quench of the hopping amplitudes in the Rice-Mele model, which is defined by

$$\mathbf{d}(k) = \gamma(1 + r\cos k, r\sin k, u) \tag{6}$$

and is depicted in Fig. 1(a). Here γ is the reference energy scale, r is the ratio between intercell and intracell hoppings, and u is the ratio between the staggered potentials on the A and B sublattices, breaking charge conjugation and chiral symmetry. We choose a quench such that $\mathcal{C}(k)$ vanishes for some k^*, a condition that, for a given H^f, is fulfilled by a vast class of initial states. Here we quench from $r^i = 0.5$ to $r^f = 2$ while keeping $u = -0.1$ constant. It is then straightforward to show that $\nu(\eta)$, which has to be zero for $\eta = 0$, increases by 2 at each critical ratio η_m^*. Such an increase by two units can be easily understood if one recognizes that the condition $\mathcal{C}(k) = 0$ is satisfied by two quasimomenta $\{k_1^*, k_2^*\}$ which, because of symmetry, are related by $k_1^* = -k_2^*$ and are thus associated with the same critical ratios η_m^*. Concurrently, the closed loop traced by $\xi_-^{(0)}(k,\eta)$ in the complex plane as a function of k touches the origin twice at the critical ratios and the winding increases by 2. Far away from η_m^* the winding of $\xi_-^{(0)}(k,\eta)$ is, instead, a robust topological invariant. Moreover, it coincides with the winding of the whole overlap function Eq. (1) since the first-order contribution $\xi_-^{(1)}(k,\eta)\delta k$ is suppressed by a factor L^{-1} and it cannot destroy the robustness of the invariant. A comparison between the loops traced by $\xi_-(k,\eta)$ for $\eta < \eta_1^*$ and $\eta_1^* < \eta < \eta_2^*$ is schematically depicted in Fig. 1(b), where the solid lines denote the finite contribution given by $\xi_-^{(0)}(k,\eta)$, while the shaded areas around them account for the L^{-1} contribution carried by $\xi_-^{(1)}(k,\eta)\delta k$.

We can now fully appreciate the interplay between a finite-dynamical winding number and a constant magnetic flux. In Fig. 2, we plot the η-dependent response of the Berry phase to an applied magnetic flux, namely, $\Delta\varphi_B(\eta)/\Phi$, where $\Delta\varphi_B(\eta) = \varphi_B(\eta;\Phi \neq 0) - \varphi_B(\eta;\Phi = 0)$ for the above specified quench in a finite Rice-Mele lattice. We compute the same quantity for different system sizes while keeping the nonzero value of the magnetic flux always equal to $\Phi/\Phi_0 = 1/10$, and we display the values of $\Delta\varphi_B(\eta)/\Phi$ in units of the universal constants $e/\hbar = 2\pi/\Phi_0$.

Increasing L at constant η, hence going towards the STSL regime, a staircase profile becomes more and more pronounced. The critical ratios at which the jumps occur are given by Eq. (3), while the heights of the different plateaus are encoded in Eq. (5). The reason is straightforward: The contribution to the Berry phase given by $\Delta\varphi_B^{(1)}(\eta)$ amounts to bounded fluctuations with zero average, which are produced by the slight mismatch between k and $k+\phi$ and are suppressed in the STSL. The contribution carried by $\Delta\varphi_B^{(0)}(\eta)$ instead corresponds to rigid shifts of $4\pi\,\Phi/\Phi_0$ each time a critical ratio is reached, independent of system size. In the proper STSL a sharp staircase profile is thus recovered.

We would like to elaborate on the differences between the TL and the STSL in terms of the Berry phase, the Wannier wave functions, and the particle current density. In the standard TL ($\eta \to 0$), the many-particle insulating state can be built out of a Slater determinant of exponentially localized Wannier functions [45]. Because a vector potential can always be gauged away for such wave functions [46], a constant magnetic flux cannot lead to observable signatures. At the same time, the time derivative of the Berry phase is linked, even out of equilibrium, to the particle current density [28]. In contrast, in the STSL regime, the localization length of the Wannier functions becomes comparable to system size [47], with a twofold implication. On the one hand, the magnetic flux can no longer be gauged away and can lead to observable signatures, such as the staircase profile depicted in Fig. 2. On the other hand, the jumps of the Berry phase at the critical ratios η_m^* are not associated with a physical current. Instead, one can show that [42]

$$\begin{aligned}\frac{d}{d\eta}\varphi_B^{(0)}(\eta) &= \frac{L}{2\pi}\int_{-\pi}^{\pi} dk\, \langle u_-^i(k)|\mathcal{J}_{DC}^f(k)|u_-^i(k)\rangle \\ &\quad + \frac{L}{2\pi}\int_{-\pi}^{\pi} dk\, \mathrm{Re}\left\{\frac{\chi_-^{(0)}(k,\eta)}{\xi_-^{(0)}(k,\eta)}\langle u_+^i(k)|\mathcal{J}_{DC}^f(k)|u_-^i(k)\rangle\right\},\end{aligned} \tag{7}$$

where $\mathcal{J}_{dc}^f(k) = v^f(k)\,\hat{\mathbf{d}}^f(k)\cdot\boldsymbol{\sigma}$ is the component of the particle current operator that commutes with the postquench Hamiltonian and describes a DC current, while $\chi_-^{(0)}(k,\eta) = \langle u_-(k+\delta k,t)|u_+(k,t)\rangle + O(L^{-1})$. In the interesting case in which the Berry phase develops a staircase profile, the first integral, which is the expectation value of the DC current and is the only contribution appearing in the long time limit of a TL system, is vanishing due to symmetry. The jumps are, instead, produced by the additional contribution in the second line of Eq. (7), which is absent in the standard TL. This integral does not correspond to the expectation value of a particle current, and it rather involves the interband elements of the DC current operator.

In summary, we have shown that intriguing topological features arise in the STSL regime after a quantum quench when both time and system size are sent to infinity while keeping their ratio finite. In particular, we have rigorously defined a dynamical winding number $\nu(\eta)$, which characterizes the many-particle state of a 1D two-band model in the STSL regime [see Fig. 1(b)]. Notably, its definition does not rely on any specific symmetry, at variance with the customary equilibrium setting. We have shown that the dynamical winding number physically encodes the linear response of the Berry phase to an applied magnetic flux, which thus exhibits a staircase behavior as a function of η (see Fig. 2). The plateaus are quantized in units of $e/\hbar$, and the jumps between them occur at the well-defined critical times given by Eq. (3). It is also worth mentioning that this phenomenon can be observed with state-of-the-art experimental techniques. The long coherence time of ultracold atoms in optical lattices [48] may also allow one to approach the STSL regime experimentally in finite systems. Moreover, given the possibility to generate artificial gauge fields [49] and reconstruct the time-dependent Berry phase through quantum state tomography techniques [19,20,30], we expect experiments with ultracold atoms, similar to the one described in Ref. [30], to enable observation of the onset of a staircase profile as depicted in Fig. 2. An alternative implementation could be based on quantum walks in photonic platforms where the present quench dynamics can be simulated and the time-dependent Berry phase can be measured [50,51]. Our work provides a starting point for investigating further topological properties unique to the STSL regime, including the study of higher dimensions with richer geometry of Bloch bands, and probing the robustness of the dynamical winding number ν to the breaking of translation invariance and its generalization in the presence of many-body interactions.

L.R. acknowledges useful discussions with L. Barbiero, R. Saint-Jalm, and I. Spielman. J.C.B. acknowledges financial support from the German Research Foundation (DFG) through the Collaborative Research Centre SFB 1143 (Project No. 247310070), the Cluster of Excellence ct.qmat (Project No. 390858490), and the DFG Project 419241108. F.D. acknowledges financial support from the Italian Centro Nazionale di Ricerca in High Performance Computing, Big Data and Quantum Computing, funded by European Union - NextGenerationEU (Grant No. CN00000013).

[1] M. Z. Hasan and C. L. Kane, Rev. Mod. Phys. **82**, 3045 (2010).
[2] C.-K. Chiu, J. C. Y. Teo, A. P. Schnyder, and S. Ryu, Rev. Mod. Phys. **88**, 035005 (2016).
[3] X.-G. Wen, Rev. Mod. Phys. **89**, 041004 (2017).
[4] K. v. Klitzing, G. Dorda, and M. Pepper, Phys. Rev. Lett. **45**, 494 (1980).
[5] D. J. Thouless, M. Kohmoto, M. P. Nightingale, and M. den Nijs, Phys. Rev. Lett. **49**, 405 (1982).
[6] F. D. M. Haldane, Phys. Rev. Lett. **61**, 2015 (1988).
[7] C. L. Kane and E. J. Mele, Phys. Rev. Lett. **95**, 146802 (2005).
[8] B. A. Bernevig, T. L. Hughes, and S.-C. Zhang, Science **314**, 1757 (2006).
[9] M. König, S. Wiedmann, C. Brüne, A. Roth, H. Buhmann, L. W. Molenkamp, X.-L. Qi, and S.-C. Zhang, Science **318**, 766 (2007).
[10] N. Goldman, J. C. Budich, and P. Zoller, Nat. Phys. **12**, 639 (2016).
[11] N. R. Cooper, J. Dalibard, and I. B. Spielman, Rev. Mod. Phys. **91**, 015005 (2019).
[12] A. Polkovnikov, K. Sengupta, A. Silva, and M. Vengalattore, Rev. Mod. Phys. **83**, 863 (2011).
[13] S. Vajna and B. Dóra, Phys. Rev. B **91**, 155127 (2015).
[14] J. C. Budich and M. Heyl, Phys. Rev. B **93**, 085416 (2016).
[15] Z. Huang and A. V. Balatsky, Phys. Rev. Lett. **117**, 086802 (2016).

[16] C. Wang, P. Zhang, X. Chen, J. Yu, and H. Zhai, Phys. Rev. Lett. **118**, 185701 (2017).
[17] C. Yang, L. Li, and S. Chen, Phys. Rev. B **97**, 060304(R) (2018).
[18] F. N. Ünal, A. Bouhon, and R.-J. Slager, Phys. Rev. Lett. **125**, 053601 (2020).
[19] N. Fläschner, D. Vogel, M. Tarnowski, B. S. Rem, D. S. Lühmann, M. Heyl, J. C. Budich, L. Mathey, K. Sengstock, and C. Weitenberg, Nat. Phys. **14**, 265 (2018).
[20] M. Tarnowski, F. N. Ünal, N. Fläschner, B. S. Rem, A. Eckardt, K. Sengstock, and C. Weitenberg, Nat. Commun. **10**, 1728 (2019).
[21] M. S. Foster, M. Dzero, V. Gurarie, and E. A. Yuzbashyan, Phys. Rev. B **88**, 104511 (2013).
[22] P. D. Sacramento, Phys. Rev. E **90**, 032138 (2014).
[23] M. S. Foster, V. Gurarie, M. Dzero, and E. A. Yuzbashyan, Phys. Rev. Lett. **113**, 076403 (2014).
[24] L. Mazza, D. Rossini, M. Endres, and R. Fazio, Phys. Rev. B **90**, 020301(R) (2014).
[25] M. D. Caio, N. R. Cooper, and M. J. Bhaseen, Phys. Rev. Lett. **115**, 236403 (2015).
[26] M. Calvanese Strinati, L. Mazza, M. Endres, D. Rossini, and R. Fazio, Phys. Rev. B **94**, 024302 (2016).
[27] D. Toniolo, Phys. Rev. B **98**, 235425 (2018).
[28] M. McGinley and N. R. Cooper, Phys. Rev. Lett. **121**, 090401 (2018).
[29] M. McGinley and N. R. Cooper, Phys. Rev. B **99**, 075148 (2019).
[30] G. H. Reid, M. Lu, A. R. Fritsch, A. M. Piñeiro, and I. B. Spielman, Phys. Rev. Lett. **129**, 123202 (2022).
[31] X. Chen, Z.-C. Gu, and X.-G. Wen, Phys. Rev. B **82**, 155138 (2010).
[32] Y. Ge and M. Rigol, Phys. Rev. A **96**, 023610 (2017).
[33] J. Motruk and F. Pollmann, Phys. Rev. B **96**, 165107 (2017).
[34] Y.-C. He, F. Grusdt, A. Kaufman, M. Greiner, and A. Vishwanath, Phys. Rev. B **96**, 201103(R) (2017).
[35] A. Keesling, A. Omran, H. Levine, H. Bernien, H. Pichler, S. Choi, R. Samajdar, S. Schwartz, P. Silvi, S. Sachdev, P. Zoller, M. Endres, M. Greiner, V. Vuletić, and M. D. Lukin, Nature (London) **568**, 207 (2019).
[36] S. Barbarino, J. Yu, P. Zoller, and J. C. Budich, Phys. Rev. Lett. **124**, 010401 (2020).
[37] M. J. Rice and E. J. Mele, Phys. Rev. Lett. **49**, 1455 (1982).
[38] J. K. Asbóth, L. Oroszlány, and A. Pályi, *A Short Course on Topological Insulators*, Lecture Notes in Physics Vol. 919 (Springer, Cham, 2016).
[39] M. V. Berry, Proc. R. Soc. London, Ser. A **392**, 45 (1984).
[40] B. Simon, Phys. Rev. Lett. **51**, 2167 (1983).
[41] T. Fukui, Y. Hatsugai, and H. Suzuki, J. Phys. Soc. Jpn. **74**, 1674 (2005).
[42] See Supplemental Material at http://link.aps.org/supplemental/10.1103/PhysRevB.107.L241402 for technical details.
[43] M. Heyl, A. Polkovnikov, and S. Kehrein, Phys. Rev. Lett. **110**, 135704 (2013).
[44] L. Rossi and F. Dolcini, Phys. Rev. B **106**, 045410 (2022).
[45] N. Marzari and D. Vanderbilt, Phys. Rev. B **56**, 12847 (1997).
[46] W. Kohn, Phys. Rev. **133**, A171 (1964).
[47] On general grounds, the correlation length is expected to grow linearly in time after the quench. In the present setting, the correlation length can also be identified with the localization length of the maximally localized single-particle Wannier functions, and the velocity of the correlation spreading is dictated by $v^f(k)$. Thus, the localization length of the Wannier functions grows linearly in time until the space-time scaling limit is reached, when it becomes comparable to the system size.
[48] T. Langen, R. Geiger, and J. Schmiedmayer, Annu. Rev. Condens. Matter Phys. **6**, 201 (2015).
[49] N. Goldman, G. Juzeliūnas, P. Öhberg, and I. B. Spielman, Rep. Prog. Phys. **77**, 126401 (2014).
[50] F. Cardano, A. D'Errico, A. Dauphin, M. Maffei, B. Piccirillo, C. de Lisio, G. de Filippis, V. Cataudella, E. Santamato, L. Marrucci, M. Lewenstein, and P. Massignan, Nat. Commun. **8**, 15516 (2017).
[51] X.-Y. Xu, Q.-Q. Wang, M. Heyl, J. C. Budich, W.-W. Pan, Z. Chen, M. Jan, K. Sun, J.-S. Xu, Y.-J. Han, C.-F. Li, and G.-C. Guo, Light: Sci. Appl. **9**, 7 (2020).